KEK-74-15

BEAD PERTURBATION MEASUREMENT FOR THE KEK LINAC CAVITY

Shoji OKUMURA and Donald A. SWENSON

MARCH 1975

NATIONAL LABORATORY FOR
HIGH ENERGY PHYSICS
OHO-MACHI, TSUKUBA-GUN
IBARAKI, JAPAN

BEAD PERTURBATION MEASUREMENT FOR THE KEK LINAC CAVITY

Shoji OKUMURA and Donald A. SWENSON*

National Laboratory for High Energy Physics
Oho-machi, Tsukuba-gun, Ibaraki-ken, Japan

Abstract

The axial electric field in the KEK linac cavity is measured by a bead perturbation method. The beat signal of around 1 kHz is generated with the rf signals from the cavity in self-excitation and from a signal generator whose output frequency is fixed. The period of the beat signal is measured by a counter in order to detect the small change in the resonant frequency of the cavity due to a bead perturbation. The counting data are transferred to a mini-computer after each period of the beat signal. The average fields of each gap are calculated in the computer and they are displayed on a storage oscilloscope. It takes about 50 seconds to complete the whole process of the measurement. The measuring system and the results obtained are described in this paper.

* On leave from Los Alamos Scientific Laboratory, New Mexico, U.S.A.

§1. Introduction

The radio-frequency field in a drift tube loaded proton linac is excited in the standing wave mode. The distribution of electric field intensity along the cavity axis is sensitive to a perturbation of the cavity boundary. The distribution of the fields is a sensitive function of the resonant frequencies of unit-cells. When designing the dimension of drift tubes, the resonant frequencies of each unit-cell have been adjusted to the same value. This can be done only in an approximate method, however, and in reality, the various perturbations to the cavity are given by dimensional errors in fabrication, rf feeders, tuners, pickup probes and so forth. Since the field intensity determines the rf phase motion of protons, it must be properly adjusted to get a design performance of the beam.

Consequently, when a proton linac is built, it is a common practice to measure the electric field along the cavity axis by a perturbation method. In general, a small metallic bead is moved along the cavity axis and the small change in resonant frequency is measured. The relative field distribution is obtained by taking the square root of the shift in frequency. The pick-up efficiencies of small magnetic probes distributed along the cavity wall will be calibrated with the results obtained by this method. The probes will be used for monitoring the field distribution in normal operations.

The KEK 20-MeV Linac tank is 94 cm in inner diameter and 15.5 m in length. There are 88 full drift tubes and two half drift tubes on the end plates. The design value of resonant frequency is 201.25 MHz. The measured unloaded Q value is 6.3×10^4. When we are going to measure the relative field distribution by the perturbation method, the peak frequency shifts in each gap will be at most 100 Hz, if a bead of 6 mm in diameter is used. The same amount of the frequency shift will be also given by a drift of atomospheric temperature in a few tens of minutes. Consequently the measurement must be done as fast possible and the measuring system must be as noise free as possible. The use of a computer is one of the best way to satisfy these requirements as reported elsewhere.(1,2)

We set up the system using a mini-computer, OKITAC 4300 and a storage scope, TEKTRONIX 611. The measurements are repeated to find the optimum tuner condition for getting the designed field distribution. The shunt impedance, the field distributions for the several higher harmonic modes and the transit-time-factors are obtained from the measurements.

§2. Design of Parameters in Measuring System

The shift of resonant frequency of the cavity is equal to the shift of the beat frequency produced by mixing the signal from the cavity in self-excitation and the signal from a signal generator. The frequency of the beat signal is measured by counting a clock signal for the duration of each cycle of the beat signal. These period data are transferred to the computer immediately at the close of each period.

The shift of frequency Δf due to a small bead perturbation is given by[3]

$$\frac{\Delta f}{f} = -\frac{3\varepsilon_0 E^2 V}{4U} , \tag{1}$$

where f is the resonant frequency without the perturbation, ε_0 the free space dielectric constant, E the electric field intensity at the position of the bead, V the volume of the bead and U the total stored energy in the cavity. The size of the bead should be as small as possible if it is consistent with a significant perturbation. If we put, for example, E = 5 MV/m for the first gap and U = 52 joule, which are the estimated values for design operation, we find that a 6 mm diameter bead will produce a 70 Hz frequency perturbation. We choose this size of the bead since the magnitude of the frequency shift well suited to the measurement technique.

When the frequency of the beat signal is too large, the number of data will be unnecessarily large and accuracy of data will be poor. If, on the other hand, the beat frequency is too small, the drift of the resonant frequency during the measuring time will be a troublesome problem, and the number of data will be too small. Taking these points into consideration, we choose the beat frequency around 1 kHz.

We fix the measuring time to be 30 sec. This means the bead speed is 0.5 m/sec since the cavity is 15.5 m long. The number of data can be estimated with these values to be about 40 for the first gap and to be about 120 for the last gap. These numbers seem to be enough to calculate the average field.

The frequency of the clock signal is fixed at 10 MHz, since it follows that the magnitudes of data are around 10^4 which is compatible with the 16 bit binary memory of the OKITAC 4300.

§3. Equipment of the Measurement

3-A. Equipment for detecting the frequency shift

The device to move the bead is sketched in Fig.1. A silk string goes through the drift tube bores and returns above the cavity forming a loop. It is stretched tightly by four reels, one of which is driven by a motor. The tension of about 5 kg is given to the string when it is put on the reels. The tension is preserved thereafter by the elasticity of the string. The bead made of aluminum is fasten on the string. The deviation of the bead position from the cavity axis due to the catenary drop is less than 1 mm, if the string is set slightly upward at the cavity ends. This does not introduce significant errors to the measurement.

The bead and the computer start at the same time and the bead is stopped automatically by the photo-electric circuit (shown in Fig.1) when it passes the last gap.

Fig.2 is a block diagram showing the period measuring system. The signal from the cavity is amplified by two amplifiers in series. One is a transitorized amplifier which is supplied with dc voltage by a battery. The other is the power amplifier, HP 230 A whose vacuum tubes are heated by a external dc source. Thus, the stability of the frequency in the self-excitation operation is obtained within 2 Hz. The signal from the cavity is mixed with the signal from the synthesizer, TR-3133 D. The output frequency of the synthesizer is adjusted to produce a beat signal of 1 kHz just prior to each measurement, since the resonant frequency of the cavity drifts with the ambient temperature during the measurement. An HP 10514A Balanced Mixer is used to extract the beat signal. The beat signal is fed into the pulse trigger circuit which produces a trigger pulse at the interval of each period of the beat signal. The pulse is led to the period measuring counter in the Computer Room by a cable 70 m in length. On recieving the pulse, the contents of the counter are transferred to a buffer memory and the counter is reset to zero in preparation for counting the next period. This sequencial procedure yields a constant 2 μsec dead time during each period, which can be corrected in the course of data processing by the computer. The counter counts a 10 MHz signal from the HP 8660A synthesizer. The 16 bit period data in the buffer memory are transferred to the computer by interrupting the computer.

3-B. Data processing by the computer

The OKITAC 4300 computer has core memory of 8 k words, where each word has 16 bits. Receiving an interrupt every millisecond, the computer reads the period data from the counter. Since this procedure requires only about 30 μsec, the remainder of the computer running time between two successive interrupts can be used to process the data or to monitor the data on the storage scope. The operation speed for addition or subtruction is as fast as about 3 μsec, but that for multiplication or division is very slow (a few msec) since our computer has no hardware option for these operations. Consequently, we had to give up the complete processing of the data during the bead running time. Instead, while reading the data, the computer stores only the data which are directly necessary for calculating the average field. To make these data fit within the available memory, four data must be reduced to one data by averaging. Since each gap has still enough numbers of these average data, this procedure does not introduce errors for evaluating the average field.

In order to support the reading, storing and processing of data, the program for processing the data must be divided into the small jobs. To check that the program and system are running properly, the time elapsed from the completion of one of the jobs to the arrival of the next interrupt, which we call spare time, is monitored and displayed on the scope.

After the bead stops, the computer continues running for an additional 30 second to process the stored data. Then, the calculated results are displayed on the storage scope.

§4. Program for Processing the Data

As mentioned in the preceeding section, the whole program consists of the program for storing the data in the memory while the bead is moving through the cavity and the program for calculating the average field after the bead stops.

4-A. Data storage program

The data storage is carried out with two steps, the first step is to store the period data for one cell in a temporary storage area and to find which data are significant for calculating the average field.

The second step is to transfer the data selected by the first step into the final storage area for each gap. Receiving the interrupt command, the computer begins to read the new period data and executes one of the small jobs in the first stop and does a divided job of the second step, and then waits the interrupt command monitoring the spare time. In the early stage of the data processing, every four data are reduced to one data by taking the average. The data are displayed on the storage scope as shown in Fig.3. The procedure of the first step is described as follows.(see Fig.4)

1. The constant number of the interrupts are neglected.
2. Eight period data are added to get the average value or the base line which is used as a measure of the unperturbed frequency.
3. The threshold value which is a sum of the base line and a constant value BBB (we set BBB to 200) is determined, and the data are stored in a temporary storage area until it exceeds the threshold in value.
4. When a period data exceeding the threshold is detected for the first time, it picks up the first in the stored data whose positions on the cavity axis are within a constant distance from the position of this period data.
5. Continues to store successively read period data and waits the period data which is less than the threshold.
6. After coming the period data described in 5, continues to store those data located within a constant distance beyond the position of this period data.

The data for one gap in the temporary storage area are always replaced by the data for the next gap as they are read. The program for the second step is simpler since its main function is only to transfer the data among the memory. The first step program proceeds in parallel with the position of the bead, but the second step program proceeds one gap behind the position of the bead. Fig.5 shows the final stored data displayed on the storage scope.

4-B. Program for calculating the average field

The relative average fields for each gap are calculated by the following relation.

$$E_n = \Sigma \sqrt{\frac{(N - N_b)N}{N_b}}\ , \qquad (2)$$

where N_b is the period data for the base line and N is the period data with the bead perturbation. The values of N and N_b are corrected for dead time (mentioned in Section 3) by adding 20 to the counting data.

§5. Results of the Measurement

5-A. The average field distribution for the accelerating mode

The average field distribution for the accelerating mode was measured many times in the process of adjusting the field to the distribution of the designed average field E_0, which is expressed by

$$E_0 = 1.5 + 0.04 \cdot L \text{ (MV/m)}, \qquad (3)$$

where L is the length from the low energy end to the gap center in meter. Its adjustment was carried out with fourteen cylindrical tuners which distribute nearly equidistantly on the cavity wall. The diameter of the tuners is 10 cm and their movable depth is 15 cm. The final result is shown in Fig.6.

Though we could not adjust the distribution completely as seen from Fig.6, a calculation of beam dynamics shows that nearly the same size of longitudinal acceptance and emittance as those of designed ones are obtained with this distribution. In future, if necessary, we expect to be able to adjust the distribution more precisely by attaching a tuning device inside the cavity.

We wanted to investigate whether the air in the cavity has some effect on the distribution by using the magnetic probes. The evacuation of the cavity was found to cause a maximum change of 3 % in the field at each end of the cavity. It is not clear whether this comes from the frequency shift due to the air or the local deformation of the cavity.

5-B. R/Q measurement

To know the required power for accelerating the protons, the ratio of shunt impedance to quality factor, R/Q was calculated from the data obtained in the previous measurement. The total wall loss P is expressed by

$$P = \sum_{n=1}^{N} \frac{1}{R_n \cdot L_n} (\int E_z dz)^2 , \qquad (4)$$

where N is the number of unit-cells (89 in our case), R_n the shunt impedance of the n'th cell in ohm/m, L_n the length of the n'th cell, the electric field strength on the axis. The integration are evaluated for each cell. Here we define the average shunt impedance $\bar{R}$ by

$$\bar{R} = \frac{1}{P} \sum_{n=1}^{N} \frac{1}{L_n} \left(\int E_z dz \right)^2 . \tag{5}$$

Using the definition of Q,

$$Q = \frac{2\pi f \cdot U}{P} , \tag{6}$$

and Eq.1 which gives the relation between the electric field intensity and the frequency shift, we get the following expression,

$$\bar{R}/Q = \frac{2}{3\pi\epsilon_0 f V} \sum_{n=1}^{N} \frac{1}{L_n} \left(\int \sqrt{-\Delta f}\, dz \right)^2 . \tag{7}$$

The term of the summation in the above equation was calculated to be 1.60×10^2 Hz·m. Therefore, we get $R/Q = 0.84 \times 10^3$ ohm/m. If we put $Q = 6.3 \times 10^4$, we get $R = 53.0 \times 10^6$ ohm/m.

Total power required for the excitation of the accelerating field without beam is approximated as follows.

$$P = \frac{1}{\bar{R}} \Sigma \frac{1}{L_n} \left(\int_{nth\ cell} E_z dz \right)^2$$

$$= \frac{1}{\bar{R}} \Sigma \frac{1}{L_n} (E_0 L_n)^2 = \frac{1}{\bar{R}} \Sigma E_0^2 L_n$$

$$\simeq \frac{1}{\bar{R}} \int E_0^2 dz .$$

If we put $E_0 = 1.5 + 0.04 \cdot z$ and integrate from 0 to 15.5 (m), we obtain

$$P = 0.968 \times 10^6 \ \text{Watt}$$

5-C. Measurements for higher harmonic modes

The cavity has the TM_{01n}-like nearby modes which are very important in the analysis on the transient field characteristics and beam loading. The resonant frequencies for several higher harmonic modes were measured and plotted in Fig.7. The field distributions for these modes were also measured by the same equipment as used for the accelerating mode. The measured period data are plotted on the storage scope as shown in Fig.8. Since there are nodes of the axial average field for the higher harmonic modes, the program described in Section (4-A) cannot be used. Therefore, the average field measurement cannot be completely processed by the same program as used for accelerating mode.

We can know the ratios of average field to peak electric field for each gap from the results for the accelerating mode. Since the ratios do not change for the higher harmonic field, the average field can be evaluate with the ratios if only the peak shift frequencies for each gap are detected. Thus, the average fields for four higher-harmonic modes which are close to the dominant mode are obtained and shown in Fig.9.

The positions of the two coupler which are to be used for the accelerating operation, are shown in Fig.9. The distributions have nearly the shape of cosine functions except that the amplitudes have a slight increase toward the high energy end. This shows the cavity may be approximately expressed by a cylindrical cavity filled uniformly with some dielectric matter in the analysis of the rf properties. We can easily see that the coupling coefficients for the first, second and third higher harmonic modes will be very small, although the coupling for the fourth will be quite strong.

5-D. Transit-time-factors

The transit-time-factors and the S-coefficients were calculated both for protons and deuterons. The transit-time-factor T_n and the S-coefficient S_n are given by

$$T_n = \frac{\int_{nth\ gap} E_z(z)\cos(k_n z)dz}{\int_{nth\ gap} E_z(z)\,dz}$$

$$S_n = \frac{\int_{nth\ gap} E_z(z)\sin|k_n z|dz}{\int_{nth\ gap} E_z(z)\,dz}$$

where $E_z(z)$ is the electric field on the axis, $k_n = 2\pi z/L_n$ for protons, $k_n = 4\pi z/L_n$ for deuterons, here L_n is the length of the n'th unit-cell, and the origin of the longitudinal coordinate for the integrations is the gap center of the n'th unit cell. The results are shown in Fig.10

and Fig.11. These values closely depend on the shapes of the electric field distribution in each gap. The number of data used for calculating these values of the first gap is 12 and the size of bead may be somewhat large for the first gap to calculate these values. These cause the results for low energy side to have some errors, but the errors will decrease as the gap length becomes larger. The effect of the bead size on the evaluation of these value must be investigated in future.

Acknowledgement

We express our sincere gratitude to J. Tanaka, H. Baba and other members of the KEK Injector group for their useful suggestions and discussions. We are also grateful to K. Ishii for his many valuable helps during this work.

References

1. C.W. Owen, C.A. Radmei, and D.E. Young: "RF-perturbation measurements in long linac cavities", IEEE Transactions on Nuclear Science, June 1967, p.286 and Proceedings of the 1966 Linear Accelerator Conference, October 3-7, 1966, p.140
2. M.A. Trump, D.R. Machen, M.A. Paciotti, E.J. Schneider, and D.A. Swenson: "Bead Perturbation Measurement", Proceedings of the 1970 Proton Linear Accelerator Conference, NAL, 1970, p.1151
3. L.C. Maier,Jr., and J.C. Slator; "Field Strength Measurements in Resonant Cavities", J. Appl. Phys. 23 1952, p.68, p.78

Figure Captions

Fig.1 A schematic sketch of the bead moving equipment.

Fig.2 A block diagram of the circuits for the bead perturbation measurement.

Fig.3 A picture of the storage oscilloscope which shows the period data of the beat signal with the bead perturbation throughout the Linac. The data are biased to display the whole data at the same time.

Fig.4 A drawing to explain the procedure in the data storage program.

Fig.5 A picture of the storagescope which shows the contents of the final storage memory area.

Fig.6 The average field distribution for the accelerating mode.
(a) A picture of the storagescope showing the final results of the average field distribution. A straight line shows the design values.
(b) A plot of the average field distribution. A straight dashed line shows the design values.

Fig.7 A plot of the resonant frequencies for several higher harmonic modes.

Fig.8 The period data with the perturbation for the higher harmonic modes. (a) first, (b) second, (c) third, (e) fourth.

Fig.9 The average field distributions for the higher harmonic modes.

Fig.10 The measured transit-time-factors for protons and deuterons.

Fig.11 The measured S-coefficients for protons (dots) and deuterons (cross).

Fig. 1 SCHEMATIC DRAWING OF BEAD MEASUREMENT

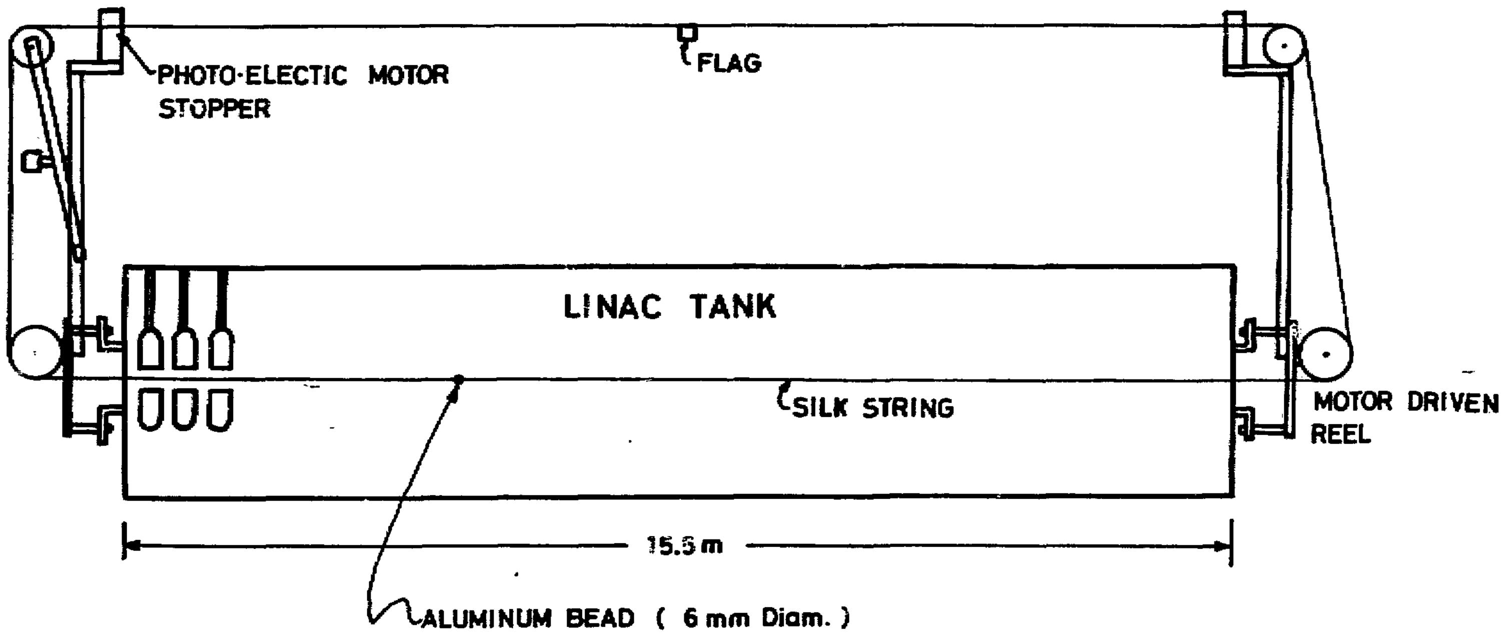

FIG. 2 FIELD MEASUREMENT BY COMPUTER TECHNIQUE

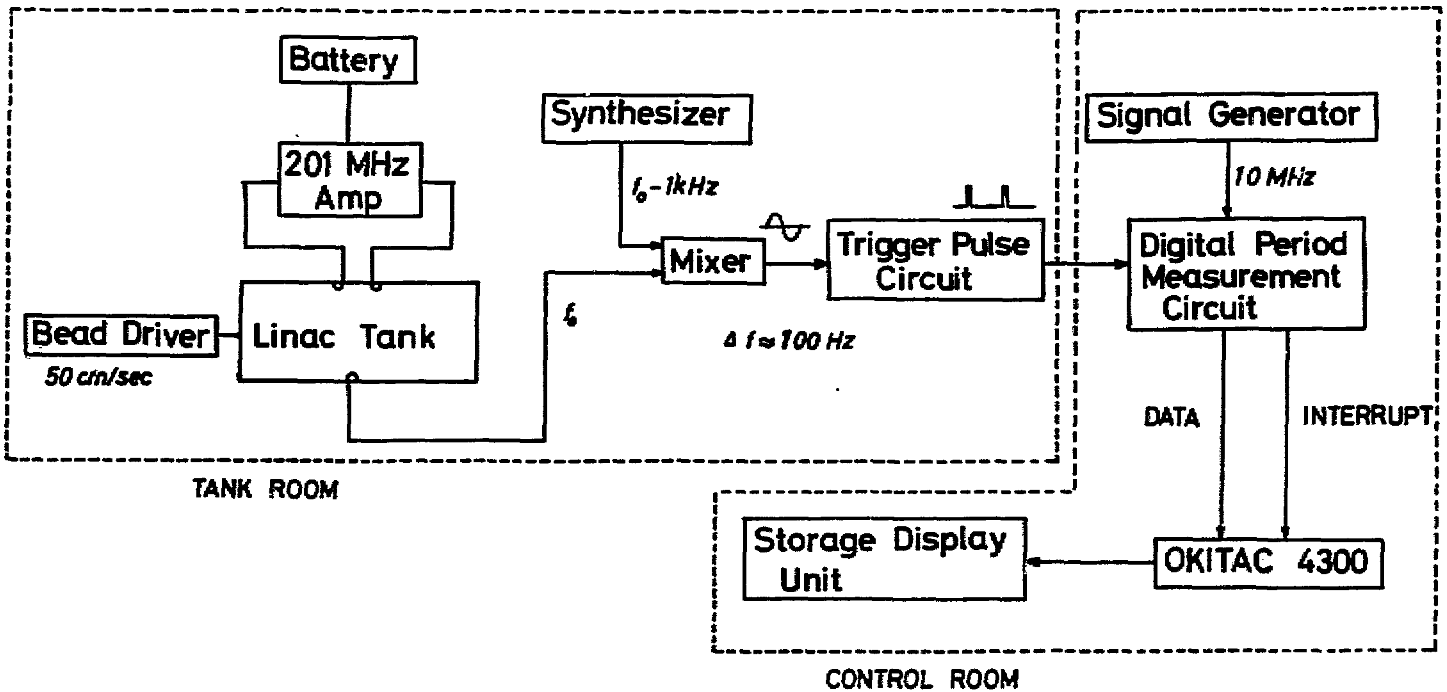

FIG. 4 DATA STORAGE PROCEDURE

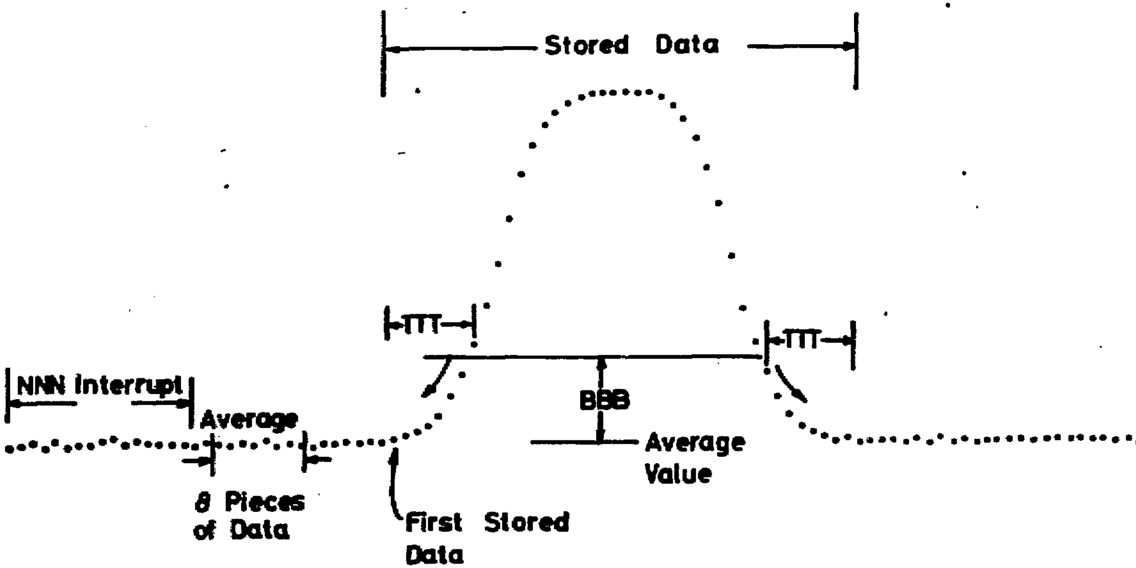

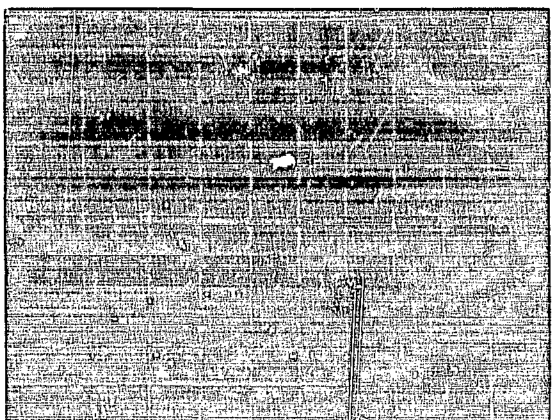

Fig. 3

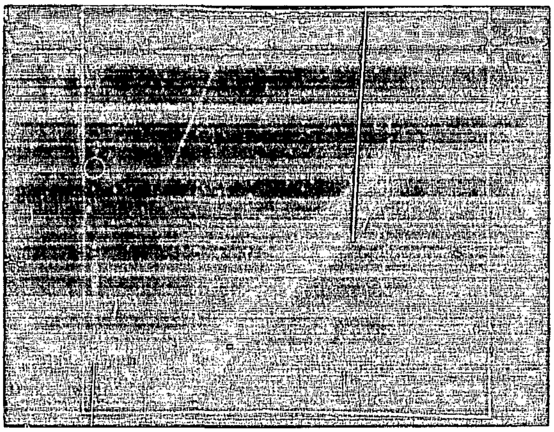

Fig. 5

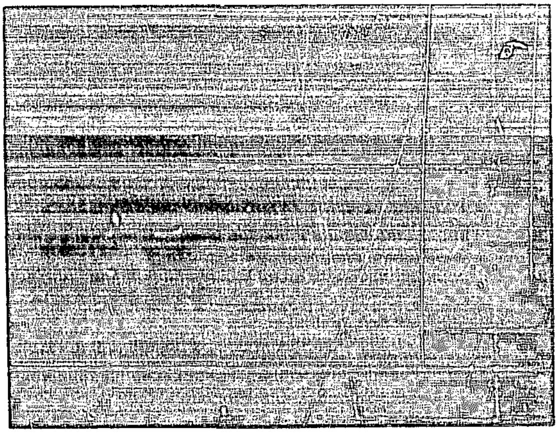

Fig. 6 (A)

Fig. 6 (b)

MEASURED AVERAGE AXIAL ELECTRIC FIELD OF ACCELERATING MODE

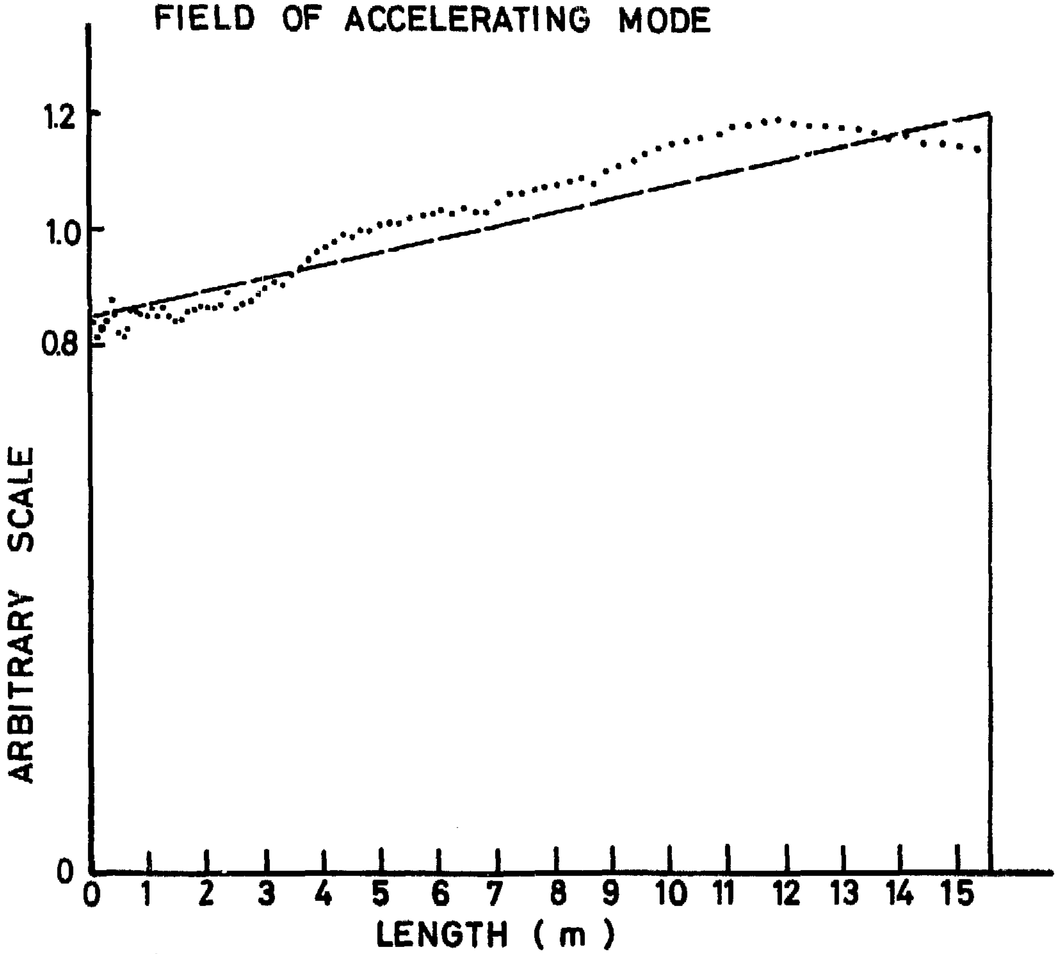

FIG. 7

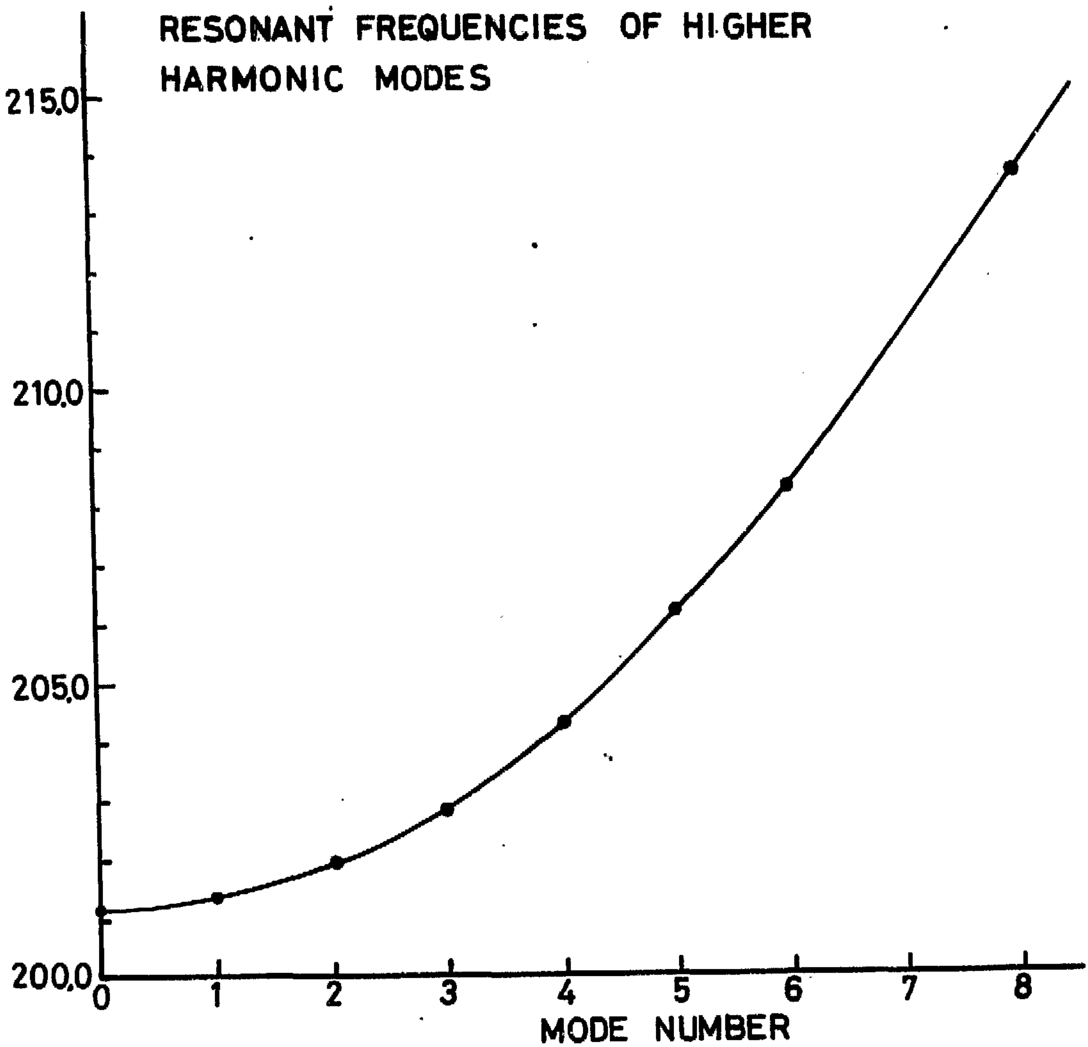

RESONANT FREQUENCIES OF HIGHER HARMONIC MODES
215,0
210,0
205,0
200,0
0
1
2
3
4
5
6
7
8
MODE NUMBER

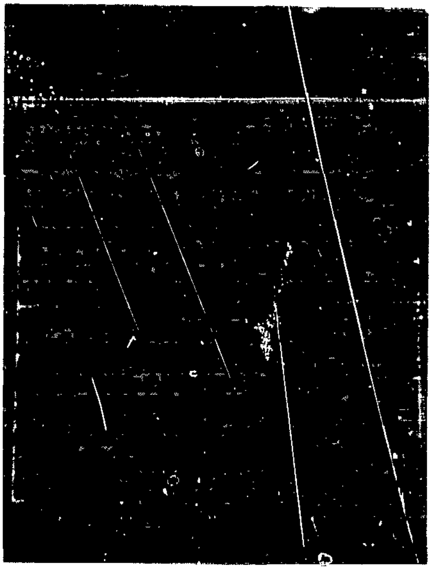

FIG. 8 (A)

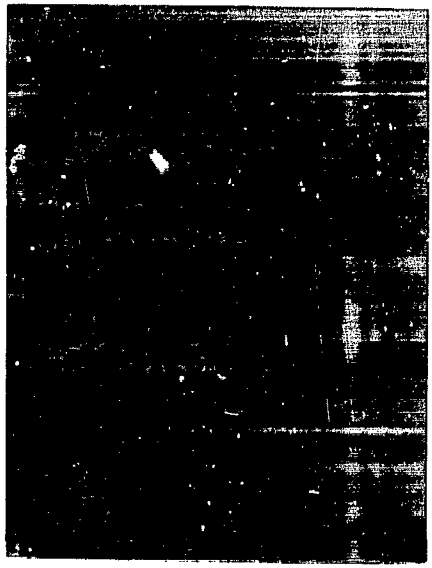

FIG. 8 (B)

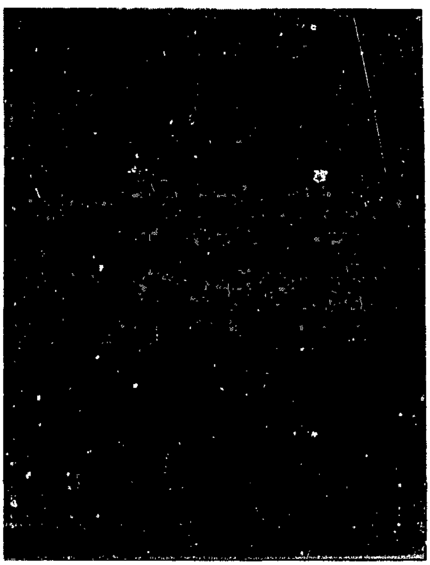

FIG. 8 (D)

FIG. 8 (E)

Fig. 9

MEASURED AVERAGE AXIAL ELECTRIC FIELD OF HIGHER MODES

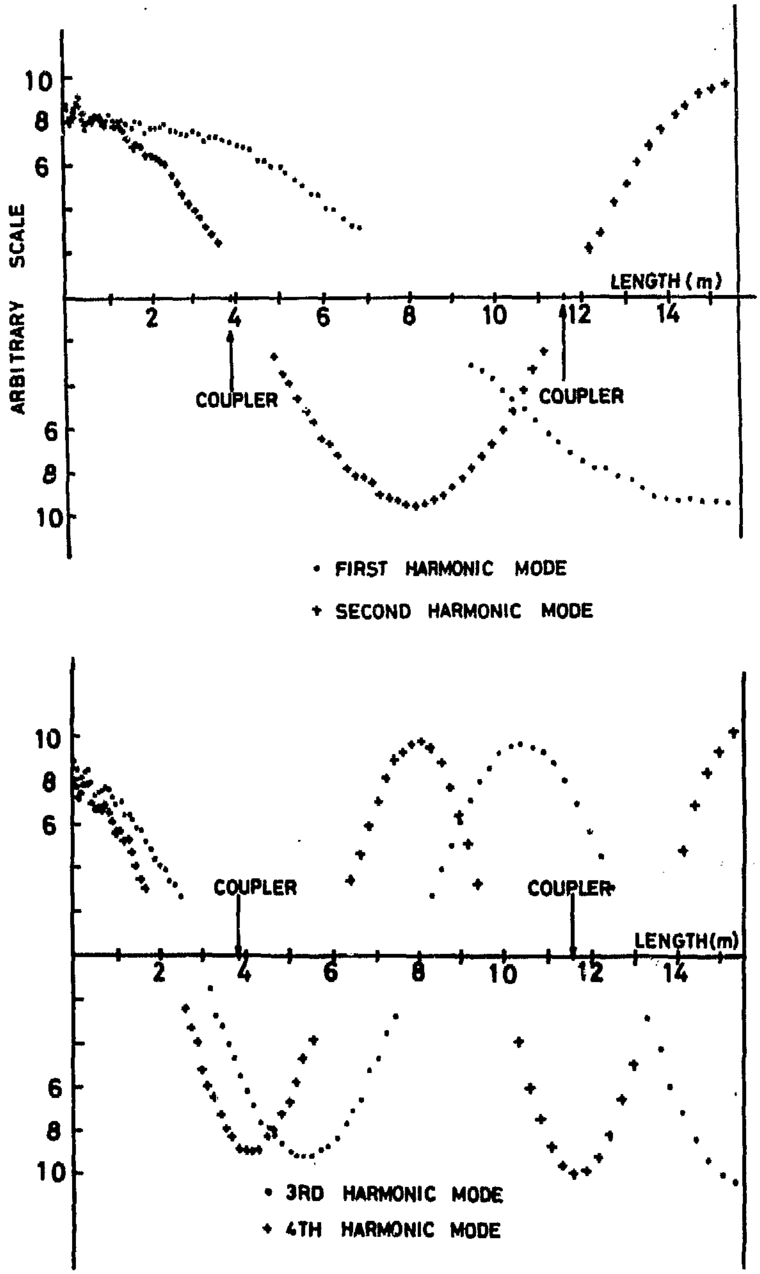

Fig. 10

MEASURED TRANSIT-TIME-FACTORS

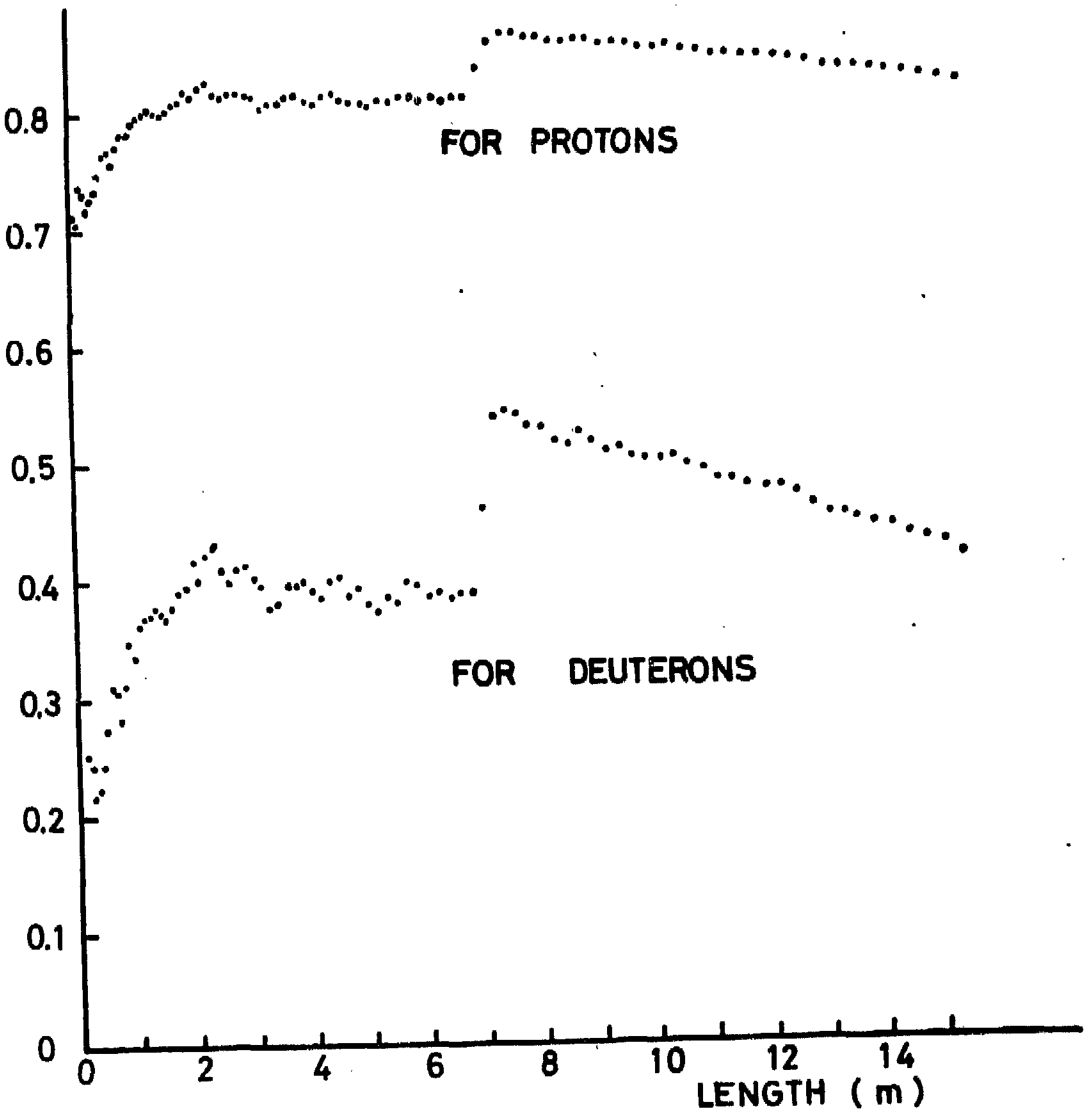

FIG. 11

MEASURED S-COEFFICIENTS